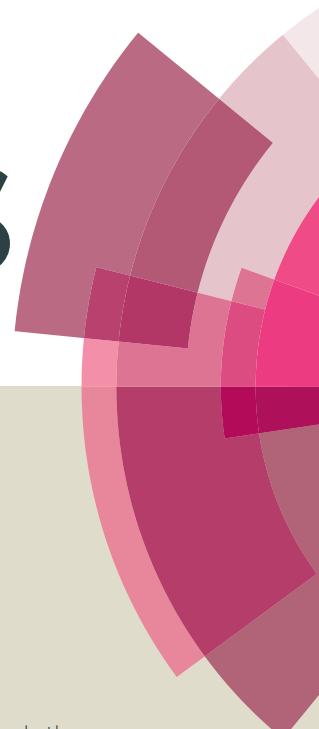


RSC Advances



This article can be cited before page numbers have been issued, to do this please use: I. Das, M. K. Mishra, S. K. Medda and G. De, *RSC Adv.*, 2014, DOI: 10.1039/C4RA10171E.



This is an *Accepted Manuscript*, which has been through the Royal Society of Chemistry peer review process and has been accepted for publication.

Accepted Manuscripts are published online shortly after acceptance, before technical editing, formatting and proof reading. Using this free service, authors can make their results available to the community, in citable form, before we publish the edited article. This *Accepted Manuscript* will be replaced by the edited, formatted and paginated article as soon as this is available.

You can find more information about *Accepted Manuscripts* in the [Information for Authors](#).

Please note that technical editing may introduce minor changes to the text and/or graphics, which may alter content. The journal's standard [Terms & Conditions](#) and the [Ethical guidelines](#) still apply. In no event shall the Royal Society of Chemistry be held responsible for any errors or omissions in this *Accepted Manuscript* or any consequences arising from the use of any information it contains.

Cite this: DOI: 10.1039/c0xx00000x

www.rsc.org/xxxxxx

ARTICLE TYPE

Durable superhydrophobic ZnO–SiO₂ films: A new approach to enhance the abrasion resistant property of trimethylsilyl functionalized SiO₂ nanoparticles on glass†

Indranee Das,^a Manish Kr Mishra,^a Samar K Medda^a and Goutam De*^a

5 Received (in XXX, XXX) Xth XXXXXXXXX 20XX, Accepted Xth XXXXXXXXX 20XX

DOI: 10.1039/b000000x

Although trimethylsilyl functionalized SiO₂ derived films show excellent superhydrophobicity, their adhesion and abrasion resistant properties are extremely poor. In this study, a new approach has been shown to improve the adhesion and abrasion properties of such films. Neutral and relatively hydrophobic [Zn(CH₃OO)₂(H₂O)₂] complex solution has been used to interact with the superhydrophobic silica gel nanoparticle dispersion. After dip-coating, the composite sol yielded films of zinc acetate/superhydrophobic silica composite network while the hydrophilic part (bonded water) associated with Zn helps in binding the hydroxyl groups (silanols) present on the glass surface. The composite films were heat-treated at 300–400 °C in nitrogen atmosphere in order to obtain transparent and superhydrophobic ZnO–SiO₂ nanocomposite films. The decomposition of zinc acetate formed ZnO nanocrystallites and remained attached with the hybrid silica matrix. These films showed excellent water repellency (water contact angle, CA≈158±7°; hysteresis ≈4°) with good adhesion and abrasion resistant properties. XRD, Raman and TEM studies confirm the existence of ZnO nanocrystallites in the composite films. Owing to the stability of hydrophobic methyl groups attached with silicon at relatively high temperature in nitrogen atmosphere, these ZnO–SiO₂ nanocomposite films remain superhydrophobic even after heat-treatment at 400 °C.

Introduction

20 Superhydrophobic coatings with different potential applications have been developed as the inspiration of some water repelling natural surfaces such as lotus leaves, water striders' leg, butterfly wings, and so on.^{1–4} Water droplets form spheres and roll off on this kind of superhydrophobic surfaces because of their unique micro-nano topography.^{1,2,5} The upper thrust force of the air entrapped in rough surface acts as the counter force against the electrostatic attraction between the water drop and hydrophilic substrate.⁶ Again, the presence of organic bulky moieties in the inorganic matrix can induce hydrophobicity into the coatings. Generally if the water static contact angle is greater than 150°, then the solid surfaces are considered as superhydrophobic. Moreover, superhydrophobicity can be understood more clearly by measuring the contact angle hysteresis value.^{7–11} Though recently many groups developed different kinds of superhydrophobic materials, but very few of them tried to solve the poor adhesion and abrasion resistant problem of these materials. Organic additives, porous characteristics and poor adhesion of the films are main constraints to induce mechanical strength and durability of superhydrophobic coatings.^{10,12} Efforts have been employed to overcome the drawback of low mechanical strength by ex-situ and in-situ insertion of metal nanoparticles into organically functionalized inorganic matrix.^{13–15} Interfacial interaction of nanoparticles with the matrix can take place by the steric and van der Waals forces which are required for ex-situ incorporation of nanoparticles;^{13,14} whereas in case of

in-situ technique, strong chemical bond between nanoparticles and host matrix are formed.¹⁵

In our previous work we fabricated trimethylsilyl functionalized superhydrophobic porous SiO₂ film (SH) on glass substrate.⁶ However, the films were suffered from very poor adhesion and mechanical strength. The poor adhesion can be understood very easily because of the absence of silanol (Si–OH) groups with the film materials. As a result, there was no possibility of bonding/interaction of the film material and hydrophilic glass surface. We attempted to control the content of silanol groups in the trimethylsilyl functionalized silica film material, however, it did not work well. In this work we have used neutral [Zn(CH₃OO)₂(H₂O)₂] complex solution to interact with the trimethylsilyl functionalized silica nanoparticulate sols. The idea behind this is that the relatively hydrophobic [Zn(CH₃OO)₂(H₂O)₂] complex^{16–18} would mix well with the hydrophobic functionalized silica, and the hydrophilic sites (bonded water) associated with Zn can make interaction/bonding with the surface hydroxyl (silanols) groups of the glass substrate. After heat-treatment, Zn acetate complex can be easily decomposed to zinc oxide (ZnO) nanocrystallites¹⁹ which can reinforce the functionalized silica superhydrophobic films as well as the film could remain adhered with the glass substrate through Zn–O–Si linkages. ZnO (formed via Zn–O–Zn bridges²⁰) is structurally similar with the silica and because of this, it is expected to be homogeneously distributed within the silica matrix. It is also noteworthy here that ZnO is well known for its non-cytotoxicity, biocompatibility and antibacterial properties.^{14,21} Recently, Zhao et al²² showed a notable

application of superhydrophobic surface with ZnO in electro-elasto-capillarity (EEC) or tap-dance of a water droplet for drug encapsulation and the actuation of microelectromechanical system devices. Hence superhydrophobic ZnO–SiO₂ nanocomposite films fabricated in this work can also find similar type of applications. Another innovative idea was employed in this work is to heat-treat the composite films in inert nitrogen gas. A relatively higher temperature is required to decompose the hydrophobic methyl groups attached with silicon in nitrogen,²³ and as a result, films got opportunity to be mechanically stronger while maintaining the superhydrophobicity. The fabricated environment friendly reinforced superhydrophobic composite films on glass were characterized by XRD, FTIR, Raman, TGA, TEM and FESEM. The abrasion resistance and water repellence abilities were investigated through standard cotton swab abrasion tests, rubbing with polishing cloths with load and water contact angle studies under different conditions, respectively.

Experimental section

Materials and Methods

All chemicals were used as received. Tetraethylorthosilicate (TEOS), 1,1,1,3,3,3-hexamethyl disilazane (HMDS) and zinc acetate dihydrate [Zn(CH₃COO)₂(H₂O)₂] were obtained from Sigma-Aldrich, while n-propanol, methanol (MeOH) and hydrochloric acid (HCl) were received from Ranbaxy fine chemicals; ammonia solution (about 25%, AR) and n-hexane were supplied by S. D. fine-chem limited. Millipore water (resistivity ~18 MΩ.cm) was used throughout this study.

Preparation of zinc incorporated methyl-modified silica sol and films

In this study methyl modified silica sol was prepared following our previously reported method⁶ with some modifications. More elaborately, 5 g TEOS was dissolved in 8 g methanol and then a mixture of 7.5 g 0.02M NH₄OH and 8.5 g methanol was added into that above mentioned solution by constant stirring. The pH of this mixture was close to 8.5–9 at this stage. After that, 3.6 ml of 0.1N HCl was added to the above mixture and stirred for additional 2 h. The whole solution was turned into gel by mixing required amount of 0.2M NH₄OH to adjust the pH near 8 and kept in oven at 60 °C for 90 min. After completion of gel formation, 25 g of methanol was added into it and again kept overnight in oven at 60 °C for ageing. To prepare organically modified SiO₂, methanol was removed from the above gel and subsequently 5 g HMDS in n-hexane (1:8 wt %) ratio was added to it and kept overnight in oven at 60 °C in closed container. Gels obtained after that, were filtered and washed once with n-hexane and twice with n-propanol. Then the washed methyl modified silica gels were dispersed by adding 45 g n-propanol applying ultrasonication to get the homogeneous dispersion.

Simultaneously, in another beaker 0.082 g of [Zn(CH₃COO)₂(H₂O)₂] was dissolved in 1 g methanol and stirred for 30 min. This solution was mixed with 4 g of above methyl-modified SiO₂ sol (SH) maintaining about 13 wt % zinc oxide with respect to equivalent silica by constant stirring for 1 h. The zinc acetate dissolved organically modified silica sol (SH-Zn) was obtained for the deposition of ZnO incorporated superhydrophobic silica films. Fabrication of the films were done

on soda lime glass substrates; prior to deposition of coatings substrates were cleaned by detergents followed by rinsing with water and isopropanol, respectively. Films were prepared by dip-coating technique (Dip-master 200, Chemat Corporation) with a withdrawal velocity of 15 cm min⁻¹ and dried at 60 °C for 1 h in an air oven. Subsequently the films were heated in 140, 300 and 400 °C in inert atmosphere (nitrogen) in a cumulating heating procedure with a ramp of 10 °C min⁻¹ for 1 h in all cases. For control experiments films maintaining 6 and 20 wt % zinc oxide with respect to equivalent silica were also prepared following the above method.

Characterizations

The thickness of the films fabricated on one side polished silicon wafer substrates, were measured by a spectroscopic Ellipsiometer (J. A. Woollam). For the evaluation of surface roughness (RMS) 5 measurements over a scan length of 3 mm were performed using a surface profilometer (Model SE-2300, Kosaka) and the average data was reported. The percentage of transmittance spectra of the films with respect to wavelength was measured using a Carry 50 Scan UV-visible spectrophotometer. Fourier transformed infrared (FTIR) spectra of the scratched off film samples (KBr pellet method) were recorded using a Nicolet 380 FTIR spectrometer with 200 scans for each samples. Raman spectra of the film materials were obtained by using Renishaw InVia Reflex Raman spectrometer with diode (785 nm) laser by using 20X objective lens. GIXRD patterns of the films deposited on glass substrate were recorded using a Rigaku SmartLab X-ray diffractometer operating at 9 kW (200 mA; 45 kV) using Cu Kα (λ = 1.54059 Å) radiation. Field emission scanning electron microscopy (FESEM) analysis of the films was done by Carl Zeiss, Germany, SUPRA-35VP instrument. Transmission electron microscopic (TEM) measurements were carried out with Technai G²-30ST (FEI) operating at 300 kV. For TEM analysis scratched off film samples were deposited on the carbon-coated Cu grid and used. Contact angle and hysteresis characteristics of the films were measured with a KRUSS GmbH instrument (easy drop DSA20E model) using 6 µl water droplets under ambient condition. The contact angle data were measured in 20 different areas and average value of the data were reported. TG measurements of the film samples were done using Netzsch TG209F3 Tarsus thermal analyser with a heating rate of 10 °C min⁻¹ in nitrogen atmosphere. Abrasion resistant tests of the superhydrophobic films were performed qualitatively following the cotton swab abrasion test.^{1,10,24,25} This test was performed in the following way. The samples were hold using adhesive tapes on a top pan weighing balance and the coated surfaces were rubbed manually along one direction by the pure cotton bud (Johnson & Johnson, USA) maintaining ~100±10 and 20±10 g of loads for SH-Zn and SH films, respectively. After abrasion the films were rated 1 to 5 according to the degree of damage. In order to check the surface hardness of the superhydrophobic nanocomposite coatings on the glass surface, the film of dimension 1.5 x 1.5 cm² was moved facing the polishing cloth surface along one direction (about 8 cm) after putting 10 and 100 g loads on the top of the film.²⁶ The test was repeated three times for the same coating sample. The changes in coating surfaces before and after each cycle of abrasion test were examined by optical microscope with a 20X magnification to observe any

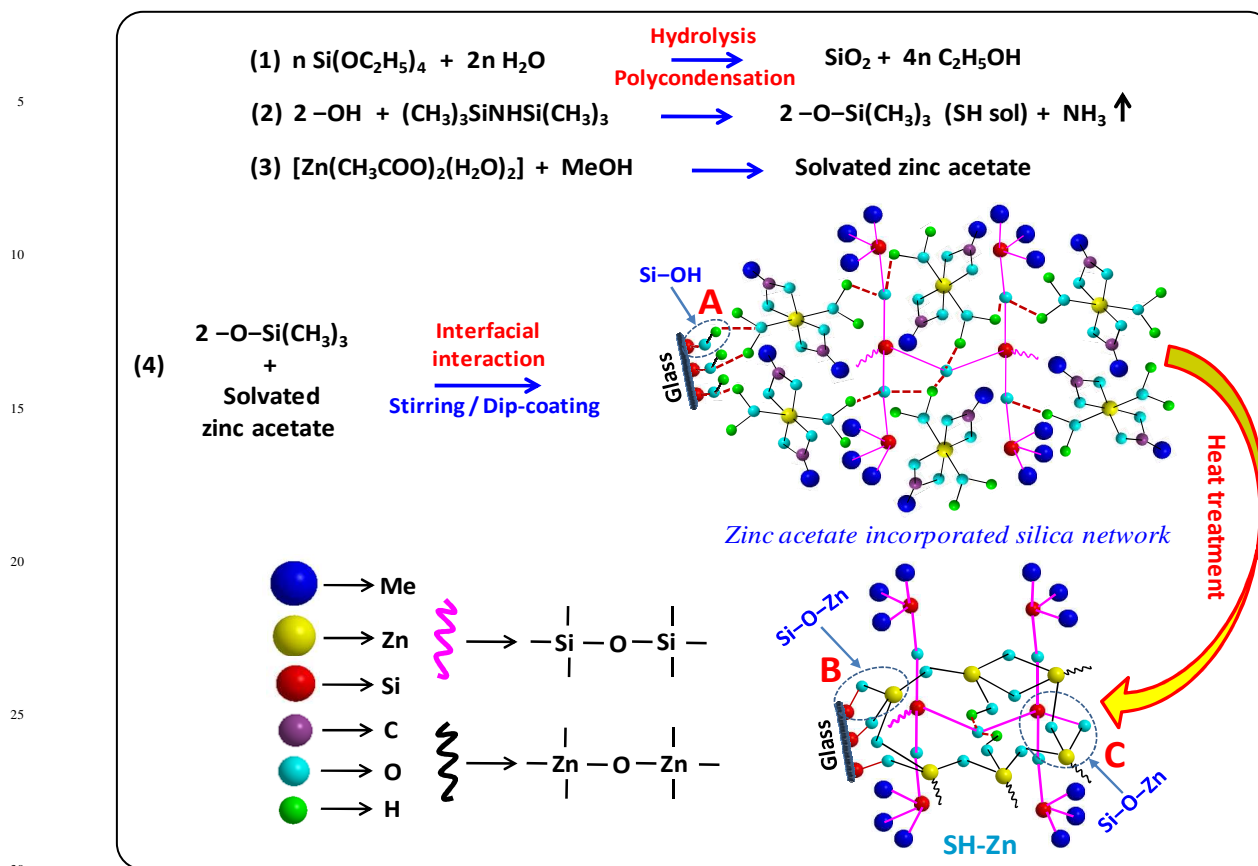


Fig. 1 Schematic representation showing the reaction scheme of zinc oxide incorporated organically modified superhydrophobic film formation.

damage and water contact angle measurements.

Results and discussion

After addition of zinc acetate complex in methanol, it was solvated. When this solution was mixed with the methyl functionalized superhydrophobic silica sol (SH), the zinc acetate molecules interacted with the organically modified silica due to its relatively hydrophobic nature, and with stirring a stable zinc acetate incorporated silica sol (SH-Zn) was resulted. About 13 wt % equivalent ZnO was maintained with respect to equivalent SiO₂. The reactions and schematic representation of the entire process are shown in Fig. 1. After dip-coating, zinc acetate complex surrounded with silica matrix formed a homogeneous layer on glass. It is expected that the hydrophilic sites associated with Zn would be in close contact with the silanol groups present on the glass substrate (see the area marked by 'A' in Fig. 1). This interaction finally induces the adhesion of the films after subsequent drying and heat-treatment stages due to the formation of Si-O-Zn linkages (see the area marked by 'B' in Fig. 1). It is noteworthy here that heat-treatment of films was done in nitrogen gas atmosphere to prevent the oxidation of hydrophobic methyl groups. During the heat-treatment zinc acetate decomposed and further polymerized into Zn-O-Zn bridges, and finally the ZnO nanocrystals are formed into the interstice of the organically modified inorganic silica network. Zn-O-Si linkages also likely to be formed in the film matrix (see the area marked by 'C' in

Fig. 1). It can be noted here that we also prepared films with compositions 6 and 20 equivalent wt % zinc oxide (with respect to equivalent silica) to compare with the film containing 13 wt % ZnO. We found that the heat treated 6 wt % ZnO incorporated coating suffered from poor adhesion possibly due to the insufficient Zn-O-Si linkages with the substrate whereas the 20 wt % showed poor transparency as well as low water repelling property due to the presence of very high content of zinc. For these reasons detailed experiments were carried out with the optimized 13 wt % zinc oxide contained SH-Zn sample.

To understand the thermal decomposition pattern for obtaining superhydrophobic films, the final sol with zinc acetate (SH-Zn) was evaporated to dryness and subjected to thermogravimetry (TG) analysis. The obtained powders were first dried at 100 °C in air and carried out TG analysis under dynamic heating condition up to 700 °C under nitrogen atmosphere (Fig. S1a, ESI†). From the TG pattern of SH it is clear that the sample did not undergo any decomposition up to 300 °C in nitrogen. In case of SH the decomposition of methyl groups starts at about 350 °C, and up to 400 °C the amount of weight loss is not very significant. On the contrary the SH-Zn shows a continuous weight loss from 100 °C onwards due to the decomposition of zinc acetate. By comparing the TG patterns of SH and SH-Zn, it can be understood that if the sample SH-Zn can be hold for some time at 300 °C, zinc acetate can be decomposed to ZnO without any deterioration of the methyl groups associated with silica.

Accordingly, the as-prepared SH-Zn powder was subjected to TG analysis with 1 h isothermal at 140, 300 and 400 °C to understand the exact percentage of decomposition in each stage (Fig. S1b, ESI†). Maximum disintegration happened by heating up to 300 °C due to the conversion of $[\text{Zn}(\text{CH}_3\text{COO})_2(\text{H}_2\text{O})_2]$ to ZnO and during 1 h isothermal at the same temperature no weight loss was observed. Further heat-treatment towards 400 °C the organic components (methyl groups) started to decompose slightly, however, no weight loss could be observed during the isothermal holding of the sample at 400 °C (Fig. S1b; ESI†). On the basis of such TG analysis, all films (SH-Zn and SH) deposited on glass substrates were heat-treated at 300 and 400 °C with 1 h holding in nitrogen atmosphere.

The quality of Zn-modified methyl-functionalized silica films were characterized in detail by several standard methods. The thickness of the films measured by ellipsiometer was estimated to be ~350 nm and the root-mean square surface roughness value (RMS) of SH-Zn film was ~46 nm. Figure 2a shows the photographs of the SH-Zn coatings on glass substrate heat-treated at different temperatures in nitrogen gas atmosphere. It shows significant increase in transparency with increasing heat-treatment temperatures to 300-400 °C. The superhydrophobic

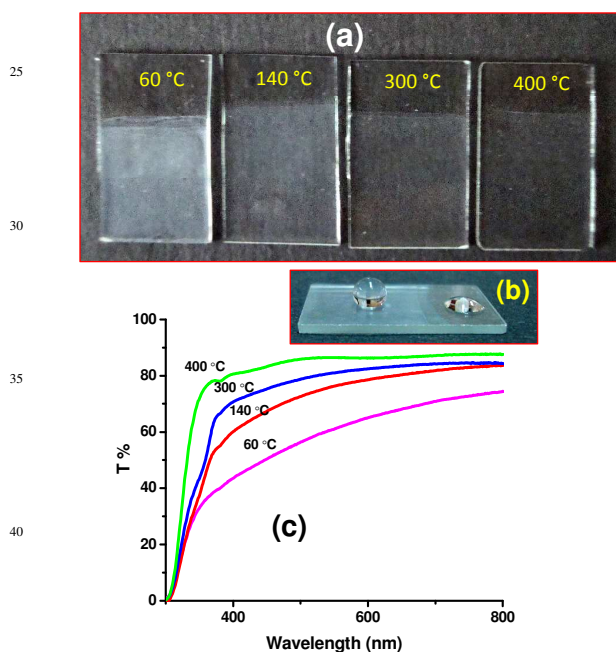


Fig. 2 Photographs showing increase in transparency of SH-Zn coatings with heat treatment (a). Image of water drops on coated and uncoated parts of glass heated at 300 °C is shown in (b). UV-Vis spectral evolution of the above coatings with respect to the heat-treatment temperatures (c).

quality of the coatings heat-treated at 300 °C is shown in Fig. 2b. Water drop forms spheres on the coated part due to non-wetting, whereas the uncoated part wets the surface. The corresponding UV-Vis spectra obtained from the above heat-treated coatings (Fig. 2a) reveal that the percentage of average transmittance in the ranges of 400-800 nm increases from 63 to 86 after heat treatment up to 400 °C (Fig. 2c; Table S1, ESI†).

With respect to temperature the incremental growth of crystalline ZnO phase in SH-Zn are clearly visible from the wide angle XRD patterns (Fig. 3). The films with partly decomposed

zinc acetate dried at 60 °C shows the crystalline peaks corresponding to zinc acetate. The formation of ZnO crystallites into the films can be observed for SH-Zn films heated at 140, 300 and 400 °C (Fig. 3). The peaks observed at 31.77, 34.43 and 36.26° 2θ, can be attributed to the (100), (002) and (101) planes of hexagonal ZnO^{15,21,27,28} (JCPDS Card No. 01-078-4493). The reference silica film (SH) without zinc acetate shows the characteristic amorphous nature (Fig. 3).

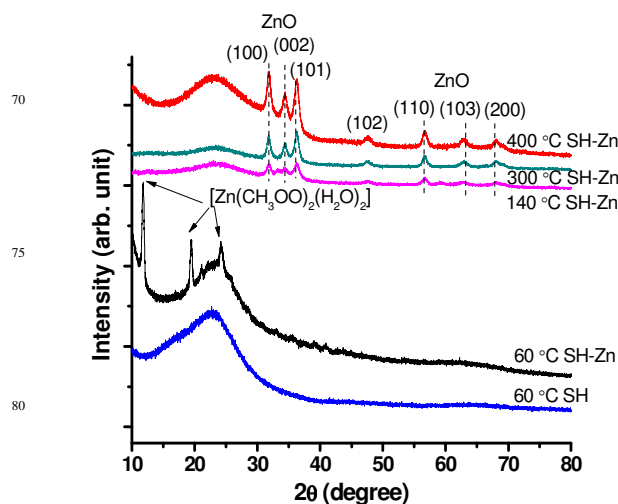


Fig. 3 Wide angle XRD patterns of SH-Zn in different heating temperatures represent the generation of crystalline ZnO in films. The film without zinc oxide precursor (SH) dried at 60 °C is also shown.

FTIR and Raman spectral analysis were performed to understand the evolution of chemical reactions with the formation of ZnO nanocrystals in the SH-Zn film materials under different heating conditions (Fig. 4). The corresponding SH films prepared without Zn was also undertaken to show the differences. The 60°C dried SH-Zn film shows existence of bands near 1578 and 1422 cm^{-1} associated with the C=O stretching vibration originated from the acetate group,²⁹ which is absent in the corresponding SH film. In case of SH-Zn the intensity of the acetate related peaks decreased with heat-treatment indicating the decomposition of zinc acetate, and films heated at 300 and 400 °C show almost absence of acetate related peaks indicating complete conversion of zinc acetate to ZnO (Fig. 4a). All films (SH-Zn and SH) show the presence of Si-O-Si originated bands at 1082 and 453 cm^{-1} (asymmetric and symmetric stretching, respectively) along with a peak at 1258 cm^{-1} for Si-C⁶ originated from the methyl modified silica matrix. It can be noted that the peaks at 2906 and 756 cm^{-1} due to the C-H stretching and CH₂ rocking mode of vibrations, respectively remain unaffected up to the heat-treatment at 300 °C under inert atmosphere. As also observed by TG analysis, 400 °C heat-treated sample shows a slight deterioration of methyl peak intensities. Nevertheless, presence of clear peaks 2906 and 756 cm^{-1} confirms the stability of methyl groups up to 400 °C. A comparative FTIR studies of the SH-Zn and SH film materials in the Si-OH stretching region (near 950 cm^{-1}) gives an idea about the relative concentration of 'Si-OH' groups present in these films. For this purpose the respective spectral regions of the 300 °C heat-treated SH-Zn and SH films have been magnified and shown in the upper inset of Fig. 4a. The SH film shows a clear absorption near 950 cm^{-1} , indicating presence of some residual

Si-OH groups even after dehydroxylation of silica gels using HMDS. However, the corresponding SH-Zn film shows relatively very weak absorption in this region and a shoulder peak $\sim 920\text{ cm}^{-1}$ (see the area marked by red dotted box in the inset of Fig. 4a) which could be originated from Zn-O-Si. This observation gives

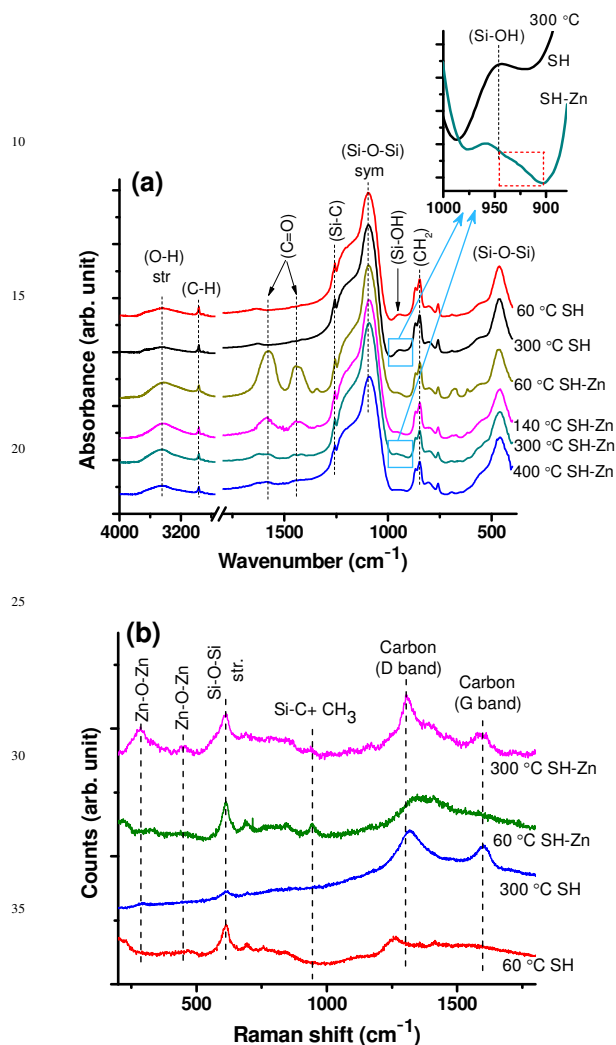


Fig. 4 FTIR (a) and Raman (b) spectra of SH-Zn and SH films heat-treated at different temperatures in nitrogen. A magnified view of the Si-O absorption region ($1000\text{--}880\text{ cm}^{-1}$) of $300\text{ }^{\circ}\text{C}$ treated SH-Zn and SH films is shown in the inset of (a).

an idea that during the decomposition of zinc acetate, it reacts also with some of the residual silanol (Si-OH) groups, and the surfaces of ZnO nanocrystallites remain bonded (Zn-O-Si) with silica. This has been shown also in the Fig. 1 schematically (see the area marked by 'C').

Raman spectra of the SH-Zn and SH films dried at $60\text{ }^{\circ}\text{C}$ and heat-treated at $300\text{ }^{\circ}\text{C}$ under nitrogen are shown in Fig. 4b. Presence of Si-O-Si stretching vibration mode near 600 cm^{-1} can be observed³⁰ in cases of both SH-Zn and SH films dried at $60\text{ }^{\circ}\text{C}$. As expected no ZnO related bands has been observed for the dried SH-Zn film. The SH-Zn film heat-treated at $300\text{ }^{\circ}\text{C}$ in nitrogen showed two clear bands near 292 and 458 cm^{-1} in Raman due to the generation of crystalline ZnO.^{27,31} Both the heat-treated films also show Si-O-Si bands near 600 cm^{-1} and a new set of carbon related 'D' and 'G' bands at 1310 and 1590

cm^{-1} , respectively. These carbon related bands are observed due to the decomposition of acetate groups under nitrogen atmosphere.³² It is noteworthy here that the presence of such graphitic carbon in the films would not affect the superhydrophobicity of the films because the graphitic carbon

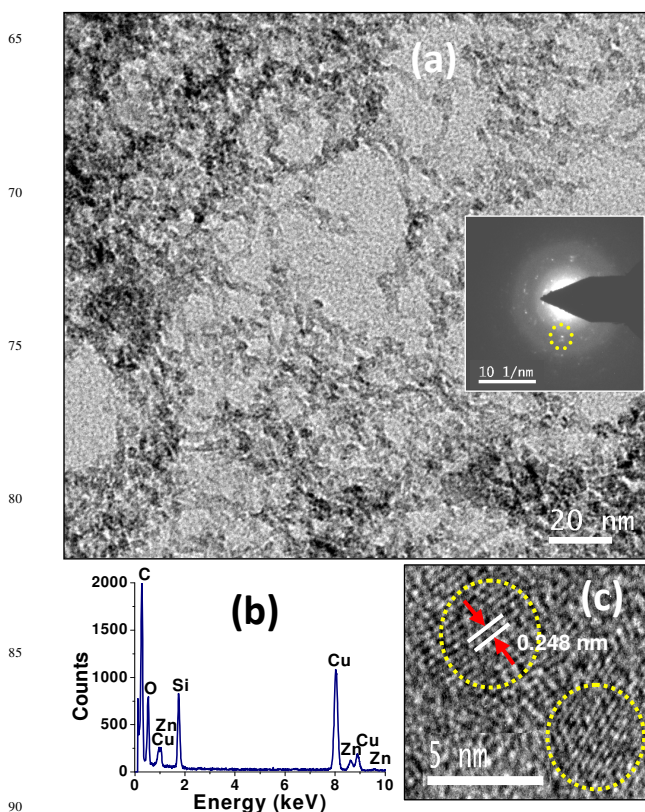


Fig. 5 TEM studies of ZnO incorporated organically modified silica (SH-Zn) film heated at $300\text{ }^{\circ}\text{C}$. Bright field image shows the network structure (a) and EDS shows the presence of Si, Zn and O elements in the film (b). SAED pattern with spots/rings and HR-TEM image showing fringes of crystalline ZnO are shown in the insets of (a) and (c), respectively.

itself hydrophobic in nature.^{33,34} We did not observe also any visual colouration or problems related to the transparency of the films due to the presence of such carbon particles.

The above studies confirmed the formation of ZnO nanocrystallites with bonding with the methyl functionalized silica network at $300\text{ }^{\circ}\text{C}$ in nitrogen atmosphere. So, the morphology of the material and distribution of crystalline ZnO in organically modified silica film matrix were investigated by transmission electron microscopic (TEM) studies. Figure 5 shows the bright field TEM micrograph of SH-Zn film heat-treated at $300\text{ }^{\circ}\text{C}$ in nitrogen. Agglomerated ZnO-SiO₂ nanocomposite particles having $\sim 10\text{ nm}$ in size in the network structure is visible in the TEM image (Fig. 5a). EDS pattern (Fig. 5b) acquired from the different portion of the TEM image shows the presence of Si, Zn and O. Signals of Cu observed in the EDS are from Cu grid used for the TEM study. HR-TEM image (Fig. 5c) reveals the formation of crystalline ZnO into this matrix which is also confirmed by the SAED pattern (inset of Fig. 5a). The d-spacing (0.248 nm) calculated from HR-TEM is well matched with the (101) plane of XRD.²⁸ A semi-quantitative analysis from the Si and Zn peaks of EDS reveals the atomic ratio of Si:Zn $\approx 8:1$,

which is close to the nominal composition used for sol preparation.

The surface topography of the SH-Zn film heated at 300 °C was also observed by FESEM (Fig. 6). Figure 6a shows the presence of rough surface topography with densely populated agglomerates. The elemental mapping was performed on the same film to check the distribution of the Zn on the SH-Zn surface. It can be clearly seen that Zn is uniformly distributed throughout the entire surface of the coating (Fig. 6b), indicating the homogeneous incorporation of ZnO into the interstice of organically modified silica matrix of the film. The superhydrophobic character of the SH-Zn surface can be explained by the Cassie-Baxter model (Fig. 6c) where the water droplets form sphere and reside on the top of the rough surface but do not fill up the nanogrooves.

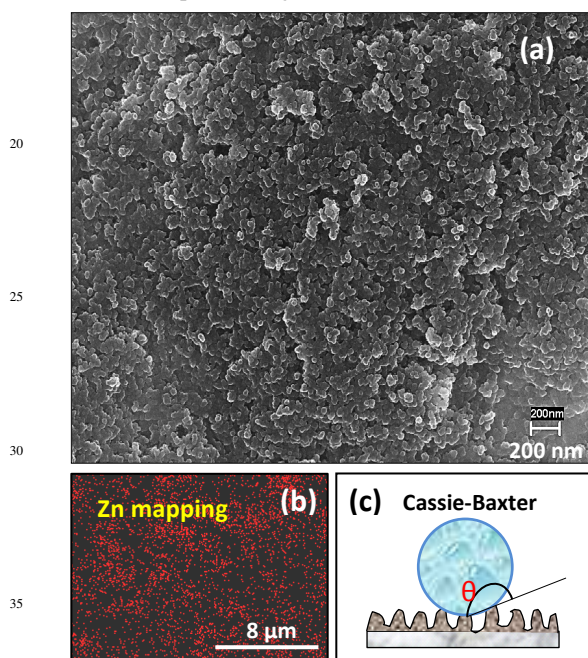


Fig. 6 (a) FESEM image showing the surface topology of SH-Zn film heated at 300 °C. (b) Elemental mapping of Zn reveals the homogeneous distribution of Zn in the entire SH-Zn film. (c) Schematic representation of the Cassie-Baxter model to show the superhydrophobic nature of film.

Due to the presence of soft organic moieties in superhydrophobic materials and high surface roughness, usually these coatings can be easily damaged by scratching and abrading. In this case, the standard abrasion test was applied to investigate the abrasion resistant property of the SH-Zn films on glass slides. The heat-treated (300 °C/nitrogen) SH-Zn and SH coatings were tested following the cotton swab abrasion test as described in the experimental section.^{1,10,24,25} According to this test, the rating criteria were as follows: rating 1-the substrate was exposed; rating 2-significant amount of material was removed, but substrate not exposed and thick abrasion line seen; rating 3-less material was removed and the abrasion line was less thick; rating 4-abrasion line was very thin; rating 5-no abrasion line observed. The SH-Zn coating showed the best result i. e. rating 5 after rubbing the surface with cotton swab by maintaining ~100±10 g load, and the rubbed area repelled water drop as before. However, the corresponding reference SH film showed rating 1

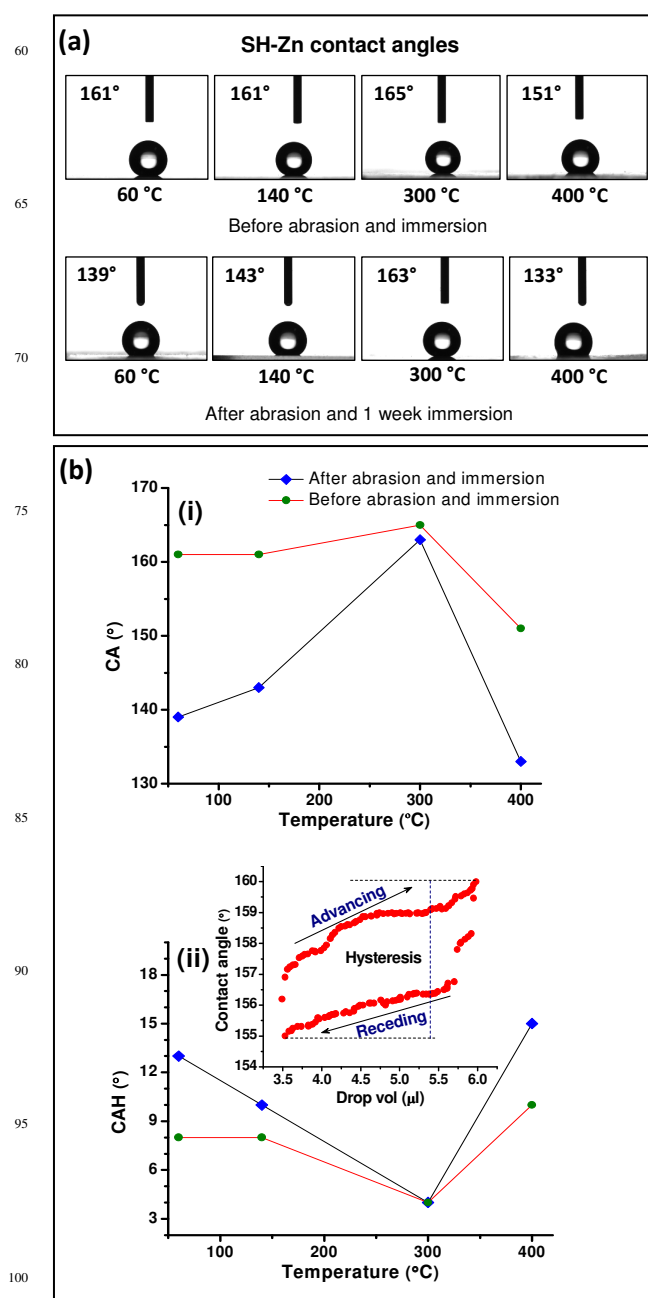


Fig. 7 (a) Images of water drops (volume 6 μ l) showing the contact angles for SH-Zn films on glass heated at different temperatures (60, 140, 300 and 400 °C) before and after abrasion and followed by immersion. (b) Plots showing the changes in contact angle (i) and hysteresis (ii) of SH-Zn films after the tests. Inset in (bii) shows the contact angle hysteresis loop of the sample heated at 300 °C.

i. e. exposed surface was wetted completely by water drop even after rubbing by applying much lower (~20±10 g) load.

The contact angle, CA (Fig. 7a,bi) and contact angle hysteresis, CAH (Fig. 7bii) of the SH-Zn films heat-treated at different temperatures were measured and the data are presented in Fig. 7. The SH-Zn film heat-treated at 300 °C showed highest CA (\approx 165°) and CAH (\approx 4°) values (Fig. 7a,b; see also the advancing and receding hysteresis loop in the inset of Fig. 7bii). Decrease of CA (\approx 151°) and CAH (\approx 10°) in case of 400 °C sample indicates decomposition of some methyl groups as also

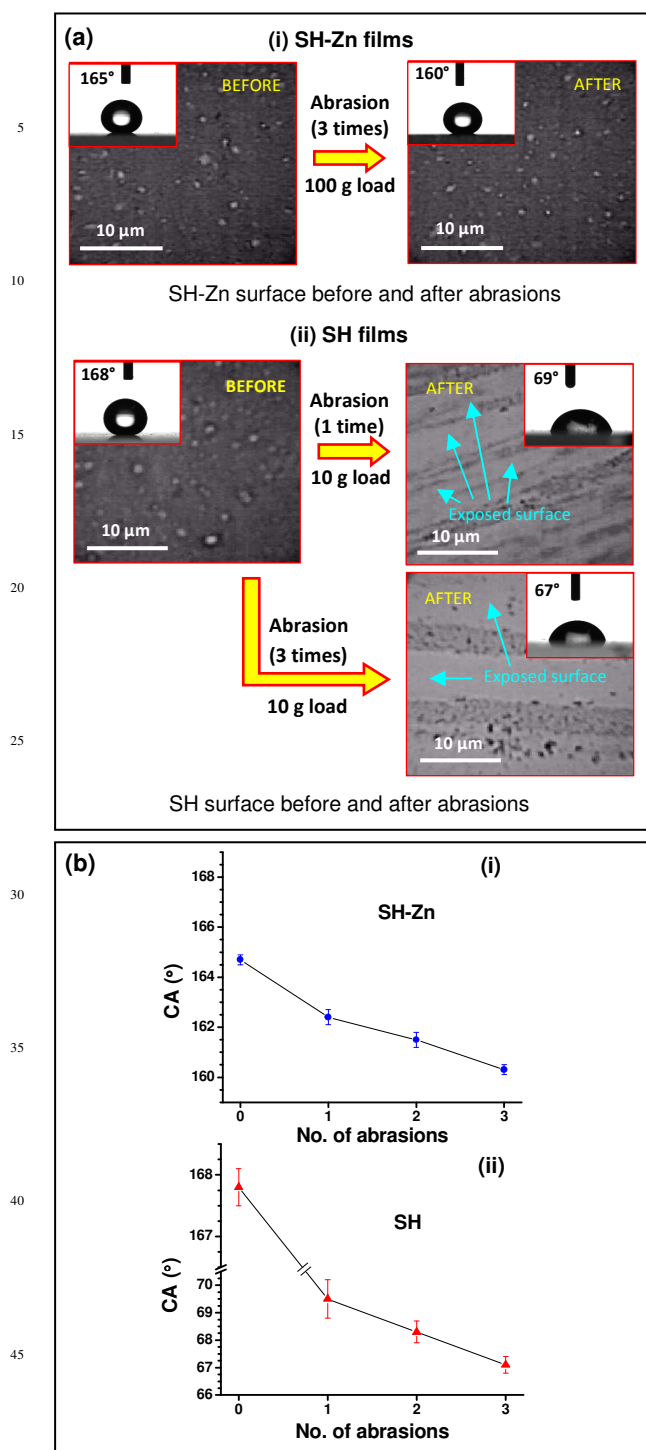


Fig. 8 (a) Images of surfaces and contact angles of water drops (volume 6 μl) on SH-Zn (i) and SH (ii) films (heated at 300 °C) before and after abrasions by polishing cloth with load. (b) Plots showing the changes in contact angles for SH-Zn (i) and the corresponding SH films (ii) before and after the same test.

confirmed by the FTIR and TG analysis. To check water repellency further, all these coated samples were subjected to cotton swab tests and followed by immersed into tap water (pH~7) for one week^{1,9}, and measured the CA and CAH values

again. The SH-Zn film (300 °C) showed almost no deterioration of CA ($\approx 163^\circ$) as well as CAH ($\approx 4^\circ$) after the abrasion test followed by 1 week of water-immersion (Fig. 7a,b). The corresponding control SH coating showed initially very high CA ($\approx 167^\circ$) became hydrophilic (CA $\approx 64^\circ$) after performing these tests (Fig. S2; ESI[†]), indicating very poor abrasion resistant property compared to the SH-Zn film heated at 300 °C. SH-Zn film samples were exposed in normal environment (temperature $\sim 32 \pm 3^\circ\text{C}$ and humidity $\sim 62 \pm 8\%$) for more than six months continuously to study the effect of outdoor dust, light and air on them,⁹ but their performances related to the superhydrophobic properties remained intact like the original coatings. The surface hardness of the heat-treated (300 °C/nitrogen) SH-Zn and SH coatings on glass was tested using polishing cloth as described in the experimental section.²⁶ After moving the SH-Zn film three times facing polishing cloth surface applying 100 g load, the polished area did not exhibit any noticeable abrasion mark and the surface showed negligible changes in contact angles during each time of polishing (Fig. 8ai,bi). On the contrary, the exposed glass surface can be clearly observed in case of the corresponding SH film after the first test cycle with much lower (10 g) load and a huge change in water contact angles (Fig. 8aii,bii) was observed.

Two things can improve the abrasion resistant properties of the superhydrophobic films (i) improvement of adhesion of the film material and (ii) reinforcing the superhydrophobic coating material. It is known that the ordinary soda-lime-silica glass contains appreciable amount of surface hydroxyl (silanol) groups^{35,36} and it is known that these groups interact easily with the hydrophilic components present in sols initially through H-bonding (see schematic Fig. 1) and followed by covalent linkages after heat-treatment through elimination of water.³⁷ In our approach addition of $[\text{Zn}(\text{CH}_3\text{COO})_2(\text{H}_2\text{O})_2]$ with trimethylsilanized silica serves dual purpose. This unique neutral complex (which can be solvated in relatively less polar solvent) has both hydrophobic (methyl) and hydrophilic (coordinate bonded H_2O with Zn) groups. So it can interact/mix well with the hydrophobically functionalized silica, as well as with the hydrophilic glass surface through H-bonding. The later formed covalent linkages through condensation reactions during subsequent heat-treatments (see Fig. 1). As a result, the adhesion quality of our coating has been improved (supported by cotton swab and polishing cloth abrasion tests). Additionally, encapsulation of ZnO nanocrystallites (supported by XRD, Raman and TEM) as well as bonding of these nanocrystals with silica network (supported by FTIR) has improved the overall hardness and mechanical durability of the film materials (supported by cotton swab rubbing followed by water immersion tests and abrasion test using polishing cloth). The excellent water repellent behaviour of the SH-Zn surface can be explained by the Cassie-Baxter model (see Fig. 6c) where the water droplets form sphere and reside on the top of the rough and compact agglomerates (supported by FESEM) but do not fill up the nanogrooves. External pressure or poor mechanical strength of the surface can convert this Cassie state into Wenzel state where liquid fill up the nanogrooves, causing decrease in superhydrophobicity.^{26,38} So robustness of the film is needed to maintain the Cassie state.²⁶ In this SH-Zn film the soft

organically modified superhydrophobic silica framework is reinforced by the in situ generation of ZnO nanocrystallites with systematic heat treatment under inert atmosphere. It is expected that this robust ZnO–SiO₂ nanocomposites will provide the stability of the Cassie state and will avoid the transition of Cassie state to Wenzel state under water pressure to maintain the superhydrophobicity for longer period of time.

Conclusions

We showed a successful new approach to improve the adhesion and abrasion resistant properties of organically modified superhydrophobic silica films on glass. Use of a neutral and relatively hydrophobic complex [Zn(CH₃COO)₂(H₂O)₂] with trimethylsilanized silica simultaneously forms bonding with the glass surface through Si–O–Zn as well as reinforce the film matrix by generating ZnO nanocrystals and making bonding with the silica network. The superhydrophobic property, good adhesion and mechanical durability were found to be optimized in case of ZnO incorporated organically modified transparent silica film (SH-Zn) heat-treated at 300 °C in nitrogen. It is expected that this type of film can also be applied on corrosion prone metals like mild steel and aluminium to protect them from getting damaged by moisture present in air.

Acknowledgements

The authors would like to acknowledge the support from CSIR (Project Nos. CSC 0114 and ESC 0202).

Notes and references

^aNano-Structured Materials Division, CSIR-Central Glass and Ceramic Research Institute, Kolkata 700032, India Fax: +91-33-24730957; Tel: +91-33-23223403; E-mail: gdc@cgcric.res.in.

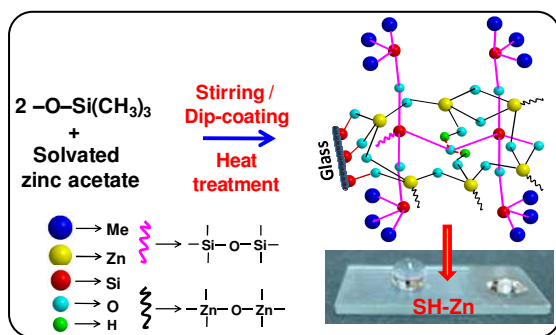
†Electronic Supplementary Information (ESI) available: Dynamic and isothermal TG analysis of SH-Zn and SH film materials (Fig. S1); contact angle images of water drops on SH coated glasses in different conditions (Fig. S2) and Table S1 showing the % transmittance data of SH-Zn coatings on glass with respect to the heat-treatment temperature under nitrogen.

- B. J. Basu and A. K. Paranthaman, *Appl. Surf. Sci.*, 2009, **255**, 4479–4483.
- Y-L. Zhang, H. Xia, E. Kim and H-B. Sun, *Soft Matter*, 2012, **8**, 11217–11231.
- B. N. Sahoo and B. Kandasubramanian, *RSC Adv.*, 2014, **4**, 22053–22093.
- M. D. Acunzi, L. Mammen, M. Singh, X. Deng, M. Roth, G. K. Auernhammer, H-J. Butt and D. Volmer, *Faraday Discuss.*, 2010, **146**, 35–48.
- H. Wang, Z. Yang, J. Yu, Y. Wu, W. Shao, T. Jiang and X. Xu, *RSC Adv.*, 2014, **4**, 33730–33738.
- D. Goswami, S. K. Medda and G. De. *ACS Appl. Mater. Interfaces*, 2011, **3**, 3440–3447.
- A. Milionis, D. Fragouli, L. Martiradonna, G. C. Anyfantis, P. D. Cozzoli, I. S. Bayer and A. Athanassiou, *ACS Appl. Mater. Interfaces*, 2014, **6**, 1036–1043.
- D. S. Facio and M. J. Mosquera, *ACS Appl. Mater. Interfaces*, 2013, **5**, 7517–7526.
- B. J. Basu and V. D. Kumar, *ISRN Nanotechnol.*, 2011, **2011**, 1–6.
- T. Verho, C. Bower, P. Andrew, S. Franssila and O. Ikkala. *Adv. Mater.*, 2011, **23**, 673–678.
- N. L. Tarwal, V. M. Khot, N. S. Harale, S. A. Pawar, S. B. Pawar, V. B. Patil and P. S. Patil, *Surf. Coat. Technol.*, 2011, **206**, 1336–1341.

- K. Jeevajothi, R. Subasri and K. R. C. Soma Raju, *Ceram. Int.*, 2013, **39**, 2111–2116.
- Z. Guo, S. Wei, B. Shedd, R. Scaffaro, T. Pereira and H. T. Hahn, *J. Mater. Chem.*, 2007, **17**, 806–813.
- J. H. Li, R. Y. Hong, M. Y. Li, H. Z. Li, Y. Zheng and J. Ding, *Prog. Org. Coat.*, 2009, **64**, 504–509.
- B-B. Wang, J-T. Feng, Y-P. Zhao and T. X. Yu, *J. Adhes. Sci. Technol.*, 2010, **24**, 2693–2705.
- T. Gordon, M. Kopel, J. Grinblat, E. Banin and S. Margel, *J. Mater. Chem.*, 2012, **22**, 3614–3623.
- T. Gordon, J. Grinblat and S. Margel, *Materials*, 2013, **6**, 5234–5246.
- W. J. Cabrera, M. D. Urzua and H. E. Rios, *J. Colloid Intr. Sci.*, 2005, **288**, 517–520.
- C-C Lin and Y-Y Li, *Mater. Chem. Phys.*, 2009, **113**, 334–337.
- P. Uthirakumar, B. Karunakaran, S. Nagarajan, E-K. Suh and C-H. Hong, *J. Cryst. Growth*, 2007, **304**, 150–157.
- U. P. Shaik, S. Kshirsagar, M. G. Krishna, S. P. Tewari, D. D. Purkayastha and V. Madhurima, *Mater. Lett.*, 2012, **75**, 51–53.
- Z. Wang, F-C. Wang and Y-P. Zhao, *Proc. Royal Soc. A*, 2012, **468**, 2485–2495.
- A. Jitianu, K. Lammers, G. A. Arbuckle-Kiel and L. C. Klein, *J. Therm. Anal. Calorim.*, 2012, **107**, 1039–1045.
- M. Xiong, J. Stein, L. Zheng, H. Lei, J. Xiao, T. Deng and Y. Zhu, *US Patent*, US 2008/0015298 (2008).
- F. G. Funderburk, E. C. Culbertson and R. G. Posey, *US Patent*, US 4493872 (1985).
- M. Gong, Z. Yang, X. Xu, D. Jasion, S. Mou, H. Zhang, Y. Long and S. Ren, *J. Mater. Chem. A*, 2014, **2**, 6180–6184.
- M. Scepanovic, T. Sreckovic, K. Vojisavljevic and M. M. Ristic, *Sci. Sinter.*, 2006, **38**, 169–175.
- M. Y. Ge, H. P. Wu, L. Niu, J. F. Liu, S. Y. Chen, Y. W. Zeng, Y. W. Wang, G. Q. Zhang and J. Z. Jiang, *J. Cryst. Growth*, 2007, **305**, 162–166.
- M. Ibrahim, A. Nada and D. E. Kamal, *Indian J. Pure Appl. Phys.*, 2005, **43**, 911–917.
- K. J. Kingma and R. J. Hemley, *Amer. Mineralogist*, 1994, **79**, 269–273.
- I. Calizo, K. A. Alim, V. A. Fonoberov, S. Krishnakumar, M. Shamsa, A. A. Balandin and R. Kurt, *Proc. of SPIE*, 2007, **6481**, 1–8.
- Y. Zhang, Y. Shen, D. Han, Z. Wang, J. Song and L. Niu, *J. Mater. Chem.*, 2006, **16**, 4592–4597.
- Y. Lin, G. J. Ehlert, C. Bukowsky and H. A. Sodano, *ACS Appl. Mater. Interfaces*, 2011, **3**, 2200–2203.
- J. Pu, S. Wan, Z. Lu, G-A. Zhang, L. Wang, X. Zhang and Q. Xue, *J. Mater. Chem. A*, 2013, **1**, 1254–1260.
- R. L. Derosa, P. A. Schader and J. E. Shelby, *J. Non-Cryst. Solids*, 2003, **331**, 32–40.
- P. F. Mcmillan and R. L. Remmele, *Amer. Mineralogist*, 1986, **71**, 772–778.
- E. Metwalli, D. Haines, O. Becker, S. Conzone and C. G. Pantano, *J. Colloid Intr. Sci.*, 2006, **298**, 825–831.
- A. Marmur, *Langmuir*, 2003, **19**, 8343–8348.

Table of contents entry:

5 Adhesion and abrasion resistant properties of the
superhydrophobic films derived from ZnO modified
trimethylsilyl functionalized SiO₂ nanocomposites have
75 been improved.



10

80

15

85

20

90

25

95

30

100

35

105

40

110

45

115

50

120

55

125

60

130

65

135